Microfluidics and Nanofluidics (2018) 22:6
https://doi.org/10.1007/s10404-017-2022-4

RESEARCH PAPER

Application of the Green function method to flow-thermoelastic forced vibration analysis of viscoelastic carbon nanotubes

Mohammad Hosseini[1] · Reza Bahaadini[2] · Mahmoud Makkiabadi[1]

Received: 30 July 2017 / Accepted: 22 November 2017 / Published online: 8 December 2017

Abstract

In this paper, the Green function method (GFM) is implemented for forced vibration analysis of carbon nanotubes (CNTs) conveying fluid in thermal environment. The Eringen's nonlocal elasticity theory is used to take into account the size effect of CNT with modeling the CNT wall–fluid flow interaction by means of slip boundary condition and Knudsen number (Kn). The derived governing differential equations are solved by GFM which demonstrated to have high precision and computational efficiency in the vibration analysis of CNTs. The validity of the present analytical solution is confirmed by comparing the results with those reported in other literature, and good agreement is observed. The analytical examinations are accomplished, while the emphasis is placed on considering the influences of nonlocal parameter, boundary conditions, temperature change, structural damping of the CNT, Knudsen number, fluid velocity and visco-Pasternak foundation on the dynamic deflection response of the fluid-conveying CNTs in detail.

Keywords Green function method · CNTs · Thermoelastic · Forced vibration · Structural damping · Knudsen number

1 Introduction

CNTs conveying fluid due to their outstanding mechanical, chemical and electrical properties have attracted worldwide attention in different applications such as fluid storages (Che et al. 1998), microfluidic and nanofluidic devices (Mattia and Gogotsi 2008), molecular and biological sensors (Yang et al. 2007) and drug-delivery devices (Bianco et al. 2005). Furthermore, it is one of the top subjects which are received great deal of attention by many researchers. For instance, Ghavanloo and Fazelzadeh (2011) investigated thermovibration and instability analysis of fluid-conveying CNT embedded in viscous fluid by using Galerkin method. Their examination determined that the eigenvalues and the related critical flow velocity could be affected by the nonlocal parameter, temperature change and structural damping of the CNT. Kiani (2013) studied vibration of embedded single-walled carbon nanotubes (SWCNTs) conveying viscous fluid based on the nonlocal elasticity theory. By using Galerkin method, he reported the effects of the small-scale parameter, inclination angle, speed and density of the fluid flow on the maximum dynamic amplitude of longitudinal and transverse displacements of the CNT. Bahaadini and Hosseini (2016a) inspected the influences of nonlocal parameter, Knudsen number, structural damping of the CNT and mass ratio on the eigenvalues and flutter flow velocity of a fluid-conveying CNT. In another study, Bahaadini and Hosseini (2016b) also scrutinized the nonlocal divergence and flutter instability analysis within CNTs conveying fluid flow. The obtained results by employed Galerkin method revealed the effects of nonlocal parameter, internal fluid flow, magnetic field and elastic foundation on the frequency and critical flow velocity of CNT. The forced vibration of CNTs containing fluid flow resting on nonlinear foundation and subjected to thermal environment has been studied by Askari and Esmailzadeh (2017) based on the nonlocal elasticity theory and surface effects. Wang et al. (2016) have investigated the dynamics of cantilevered CNTs conveying fluid subjected to longitudinal magnetic field using the differential quadrature method. Acoustic nanowave absorption through clustered fluid-conveying CNT has been studied by Zhang et al. (2016). The quantum effect on the microfluid-induced vibration of a nanotube in thermal environment has been performed by

✉ Mohammad Hosseini
hosseini@sirjantech.ac.ir; moh_hosseini@yahoo.com

[1] Department of Mechanical Engineering, Sirjan University of Technology, Sirjan 78137-33385, Islamic Republic of Iran

[2] Department of Mechanical Engineering, Shahid Bahonar University of Kerman, Kerman, Islamic Republic of Iran

Zhang et al. (2017). The influences of nonlocal parameter, fluid velocity, mass ratio, visco-Pasternak medium, follower forces and surface effects on flow-induced flutter instability of CNTs have been performed by Bahaadini et al. (2017b). The various researchers modified flow velocity of nanoflow to analyze the slip boundary conditions between the flow and wall of nanotube (Bahaadini et al. 2017a; Hosseini et al. 2014; Mirramezani and Mirdamadi 2012; Rashidi et al. 2012; Sadeghi-Goughari and Hosseini 2015). Furthermore, some works regarding vibration analysis of CNTs could be found in the literature (Habibi et al. 2016; Hosseini et al. 2014, 2016a; Mohammadimehr et al. 2017; SafarPour and Ghadiri 2017; Zeighampour et al. 2017).

In many studies, various methods have been implemented to solve the mechanical problem, such as Galerkin method (Askari et al. 2013; Jafari et al. 2017), Ritz method (Lei et al. 2013; Mirzaei and Kiani 2016), Levy-type solution method (Hosseini et al. 2016b, c, d; Jamalpoor et al. 2017a, b), boundary element method (BEM) (Liu and Chen 2003; Liu et al. 2005, 2008), finite element method (FEM) (Husson et al. 2011; Tserpes and Papanikos 2005), Adomian decomposition method (Sweilam and Khader 2010), differential quadrature method (DQM) (Ansari et al. 2016; Ghorbanpour Arani et al. 2013; Hosseini et al. 2017a, b; Xia and Wang 2010), differential transfer method (DTM) (Hosseini and Sadeghi-Goughari 2016) and Green function method (GFM) (Li and Yang 2014).

In current study, the GFM is used to examine the dynamic deflection of viscoelastic CNTs conveying fluid subjected to different boundary conditions and thermal environments. The Green function method is a powerful tool for theoretical studies of various types of problems, but there are very limited studies in the literature that use this effective method to analysis the mechanical behavior of nano-/microscale structures. Based on the GFM, the third-harmonic susceptibility of zigzag CNTs was studied by Rezania and Daneshfar (2012). Yan et al. (2013) described the linear hydrodynamic nonlocal response of arbitrarily shaped nanowires in arbitrary inhomogeneous backgrounds via Green's function surface-integral method. Mehdipour et al. (2012) determined the Green's function for an infinitesimal horizontal electric dipole on a dielectric slab over a carbon-fiber composite ground plane having anisotropic conductivity. The GFM was applied to investigate the coefficient of thermal expansion in single-walled CNT and graphene by Jiang et al. (2009). In a related work in macroscale, Kukla and Zamojska (2007) examined free vibration of axially loaded stepped beam by using GFM. Based on the Laplace transform method and GFM, the Timoshenko beam model with various boundary conditions, Li et al. (2014) examined the forced vibration of beams with damping effects. Combination effects of frequency of harmonic force and internal moving fluid flow on the forced vibration of pipes conveying fluid under different boundary conditions were studied by Li and Yang (2014). In their study, by exploiting the Euler–Bernoulli beam theory, the problem was examined in the context of classical continuum theory via GFM. Zhao et al. (2015) analyzed the coupling effects between temperature and displacement fields through analytical solutions. For this purpose, the GFM and superposition principle is employed to solve the coupled thermoelastic vibration equations of a beam. Zhao et al. (2016) proposed a GFM to obtain closed-form expressions for the mechanical behavior of cracked Euler–Bernoulli beams. Chen et al. (2016) investigated forced vibration of Timoshenko beam model under axial forces. To this end, the GFM was implemented to solve a generalized equation of motion and the dynamic deflection and rotating angle for a beam with different supported ends. According to the classical circular plate theory and GFM, Ghannadiasl and Mofid (2016) studied free vibration of stepped plates embedded in a Winkler medium by consideration of internal elastic ring support.

A scrutiny of the literature reveals that the vibration and dynamic deflection of CNTs conveying fluid flow have been fairly well studied in the context of various numerical solutions. Some of investigation has been performed on the forced vibration analysis of various beam models using GFM. However, no inclusive study on the exact solution for flow-thermoelastic forced vibration analysis of CNTs with various boundary conditions by means of GFM has been covered so far. To this end, the CNT is modeled according to the nonlocal viscoelastic Euler–Bernoulli beam theory under various boundary conditions. By considering the interaction forces of the fluid flow on the CNT, the equation of motion is obtained in the framework of the Eringen's nonlocal elasticity theory and slip boundary conditions and then is solved by using GFM. The influences of nonlocal parameter, fluid velocity, Knudsen number, temperature change, structural damping of the CNT, elastic foundations and boundary conditions on the maximum values of dynamic displacements of system are discussed.

2 Preliminary

Figure 1 shows a schematic view of a fluid-conveying CNT of thickness h, outer radius R_o, inner radius R_i, length L and flexural rigidity EI. The CNT is supported by a visco-Pasternak medium which is assumed to be continuously connected to the CNT and is subjected to a harmonic force p at position l. Consider the Cartesian coordinate system (x, y, z) with the x-axis along the length of the deflected CNT, the z-axis along the neutral axis and the y-axis along the transverse direction. The transverse CNT displacement at the axial coordinate x and time t is shown by $w(x, t)$. The governing equations of motion (Eq. (1)) and the related boundary

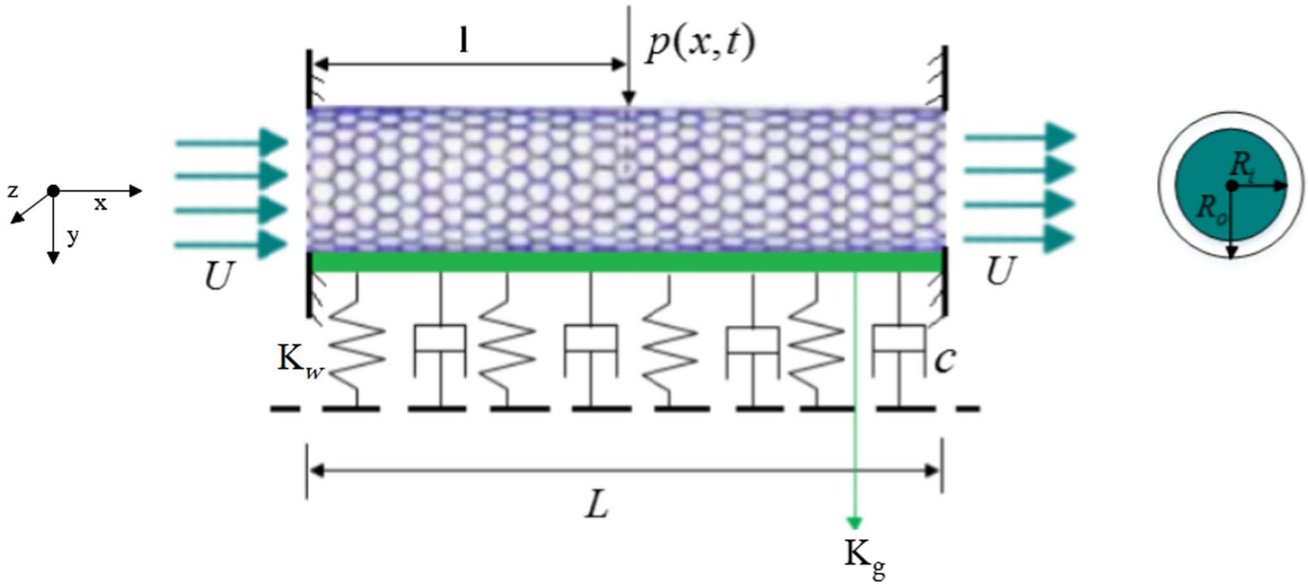

Fig. 1 Viscoelastic CNTs conveying fluid embedded in visco-Pasternak foundation

conditions (Eq. (2a–2b)) based on viscoelastic CNTs conveying fluid using nonlocal Euler–Bernoulli beam theory and considering visco-Pasternak foundation will be attained as (Arani and Amir 2013; Bahaadini and Hosseini 2016a; Ghavanloo and Fazelzadeh 2011):

$$\mathrm{EI}\left(1+g\frac{\partial}{\partial t}\right)\frac{\partial^4 w}{\partial x^4}+\left(1-(e_0a)^2\frac{\partial^2}{\partial x^2}\right)\left[\left(MU^2_{\mathrm{avg,slip}}-N^{\mathrm{T}}-K_{\mathrm{G}}\right)\frac{\partial^2 w}{\partial x^2}+2MU_{\mathrm{avg,slip}}\frac{\partial^2 w}{\partial x\partial t}+(M+m)\frac{\partial^2 w}{\partial t^2}+C\frac{\partial w}{\partial t}+K_{\mathrm{w}}w-p(x,t)\right]=0 \tag{1}$$

$$\mathrm{EI}\left(1+g\frac{\partial}{\partial t}\right)\frac{\partial^2 w}{\partial x^2}-(e_0a)^2\left[\left(MU^2_{\mathrm{avg,slip}}-N^{\mathrm{T}}-K_{\mathrm{G}}\right)\frac{\partial^2 w}{\partial x^2}+2MU_{\mathrm{avg,slip}}\frac{\partial^2 w}{\partial x\partial t}+(M+m)\frac{\partial^2 w}{\partial t^2}+C\frac{\partial w}{\partial t}+K_{\mathrm{w}}w-p(x,t)\right]=0 \text{ or } \frac{\partial \delta w}{\partial x}=0 \tag{2a}$$

$$-\mathrm{EI}\left(1+g\frac{\partial}{\partial t}\right)\frac{\partial^3 w}{\partial x^3}+(e_0a)^2\left[\left(MU^2_{\mathrm{avg,slip}}-N^{\mathrm{T}}-K_{\mathrm{G}}\right)\frac{\partial^3 w}{\partial x^3}+2MU_{\mathrm{avg,slip}}\frac{\partial^3 w}{\partial x^2\partial t}+(M+m)\frac{\partial^3 w}{\partial x\partial t^2}+C\frac{\partial^2 w}{\partial x\partial t}+K_{\mathrm{w}}\frac{\partial w}{\partial x}-\frac{\partial p(x,t)}{\partial x}\right]+\left(N^{\mathrm{T}}+K_{\mathrm{G}}\right)\frac{\partial w}{\partial x}=0 \text{ or } \delta w=0 \tag{2b}$$

where M and m are the mass per unit length of fluid and the CNT, respectively, and K_{w}, K_{G} and C denote the Winkler, Pasternak and damping of visco-Pasternak foundation, respectively. Also, e_0 is a material constant, and a is the internal characteristic length. Therefore, e_0a shows the nonlocal parameter that includes the small-scale effects into the constitutive equations for forced vibration of CNT. As indicated in Eqs. (1) and (2a), nonlocal elasticity theory is strongly dependent on the proper value of the nonlocal parameter. However, it was found that various parameters such as crystal structure in lattice dynamics, mode shapes, aspect ratio and boundary conditions have a considerable effect on the appropriate values of nonlocal parameter (Ansari and Sahmani 2012; Duan et al. 2007; Hu et al. 2011; Narendar and Gopalakrishnan 2011). Therefore, choice of the optimized value for nonlocal parameter is crucial to calibrate the non-locality effect, whereas there are no experiments conducted to obtain the value of nonlocal parameter. Details of the various values of nonlocal parameter as described by various researchers can be found in Ansari and Sahmani (2012), Duan et al. (2007), Ghavanloo and Fazelzadeh (2016) and Narendar and Gopalakrishnan (2011). For CNTs and graphene sheets, the range of $e_0a = 0$–2 nm has been widely used because the exact value of the nonlocal parameter is not known (Karlicic et al. 2015; Tiwari 2013; Wang et al. 2006).

In addition, g is viscoelastic structural damping coefficient of Kelvin's model on elastic material. This viscoelastic properties, as reported by Xu et al. (2010), may be due to zipping–unzipping mechanism between CNT and CNT contacts which lead to energy dissipation. Some additional mechanism of energy dissipation may also be happen and causes viscoelastic damping properties in CNTs (Gogotsi 2010).Viscoelastic damping may also denote certain polymer matrix, van der Waals forces or other external damping effects. So, the vibration of CNTs conveying fluid can be repressed by counting viscoelastic damping properties. Thus, the size-dependent effect and viscoelastic behavior of CNT structure may be more realistic due to the presence of energy dissipation problem at nanoscales.

There are very limited direct experimental data on the viscoelastic properties of the CNT. However, a number of researchers have reported the quality factor Q (the inverse of the energy dissipation) in CNT (Lassagne et al. 2008; Qian and Zhou 2011; Sazonova et al. 2004). Based on the viscoelasticity model represented by Kelvin model, the Q factor can be defined as ratio between the storage and loss modulus in a viscoelastic material which is related to a measure of structural damping (Zhou et al. 2011). The CNT with high-quality factors has lower rate of energy loss relative to the stored energy so that they have low damping. It was found that chirality had no noticeable effect on the CNT viscoelastic properties, while they are strongly dependent on the tube radius of CNTs in which Q factor is reduced with increase in CNT radius (Qian and Zhou 2011; Zhou et al. 2011). For CNT with tube diameters in range of 1–4 nm, Sazonova et al. (2004) reported that Q factor is in the range of 40–200 for a resonant frequency 55 MHz.

While the CNT ends are restrained both axially, a thermal axial force N^{T} will be induced in the structure due to temperature changes as:

$$N^{\mathrm{T}} = -\frac{EA}{1-2v}\alpha_x \Delta T \tag{3}$$

where A is the cross-sectional area, v is Poisson's ratio, α_x denotes the coefficient of thermal expansion in the direction of the x-axis and ΔT is temperature change. Based on the thermal elasticity mechanics theory, the Young's modulus of CNT is insensitive to temperature change in the tube when the temperature is lower than approximately 1100 K (Hsieh et al. 2006). Furthermore, it is apparent that Poisson's ratio increases with temperature although the augmentation is limited and can be measured constant at temperatures between 300 and 1200 K (Scarpa et al. 2010). Moreover, the temperature dependence of radial and axial coefficient of thermal expansion has been studied by Hwang (2004) and it was concluded that coefficients are negative at low or room temperature and become positive at high temperature.

In addition, it should be mentioned that in nanoscale, Rashidi et al. (2012) developed a modified nanotube that incorporates nanoflow viscosity and slip boundary condition. With considering the Knudsen number, one can model the slip boundary conditions between the nanoflow and walls of nanotube properly. It should be noted that Knudsen number, i.e., the ratio of the molecular mean free path length to a representative physical length scale, can be used to identify flow regime: (1) $0 < Kn < 10^{-2}$ for continuum flow regime; (2) $10^{-2} < Kn < 10^{-1}$for slip flow regime; (3) $10^{-1} < Kn < 10$ for transition flow regime; and (4) $Kn > 10$ for free molecular flow regime (Karniadakis et al. 2005). For CNTs conveying fluid, it could be possible that Kn be larger than 10^{-2}. Therefore, by considering Knudsen number, the flow velocity can be expressed as $U_{\mathrm{avg,slip}} = \mathrm{VCF} \times U_{\mathrm{avg,(no\text{-}slip)}}$ where $U_{\mathrm{avg,slip}}$ and $U_{\mathrm{avg,(no\text{-}slip)}}$ are the average fluid velocities through nanotube with slip boundary conditions and without slip boundary conditions, respectively. Also, VCF is the average velocity correction factor, which is described in more detail in "Appendix 1".

Hereafter, for simplicity, the following dimensionless quantities are defined:

$$\begin{aligned}
&\xi = \frac{x}{L}, \quad \eta = \frac{w}{L}, \quad \mu = \frac{e_0 a}{L}, \quad \ell = \frac{l}{L}, \quad \tau = \sqrt{\frac{\mathrm{EI}}{(M+m)}}\frac{t}{L^2},\\
&u = \sqrt{\frac{M}{\mathrm{EI}}}v_{\mathrm{avg(no\text{-}slip)}}L, \quad \beta = \frac{M}{M+m},\\
&N = \frac{N^{\mathrm{T}}L^2}{\mathrm{EI}}, \quad c = \frac{CL^2}{\sqrt{\mathrm{EI}(M+m)}},\\
&\alpha = \sqrt{\frac{EI}{(M+m)}}\frac{g}{L^2}, \quad \omega = \sqrt{\frac{(M+m)}{\mathrm{EI}}}\Omega L^2,\\
&q(\xi,\tau) = \frac{p(x,t)L^3}{\mathrm{EI}}, \quad k_{\mathrm{w}} = \frac{K_{\mathrm{w}}L^4}{\mathrm{EI}}, \quad k_{\mathrm{G}} = \frac{K_{\mathrm{G}}L^2}{\mathrm{EI}}
\end{aligned} \tag{4}$$

Therefore, the non-dimensional governing equations of motion and the associated boundary conditions of the CNT with considering velocity correction factor VCF can be stated as:

$$\begin{aligned}
&\left(1+\alpha\frac{\partial}{\partial\tau}\right)\frac{\partial^4\eta}{\partial\xi^4} + \left(1-\mu^2\frac{\partial^2}{\partial\xi^2}\right)\left[\left((\mathrm{VCF}\times u)^2 - N - k_{\mathrm{G}}\right)\frac{\partial^2\eta}{\partial\xi^2}\right.\\
&\left. + 2(\mathrm{VCF}\times u)\sqrt{\beta}\frac{\partial^2\eta}{\partial\xi\partial\tau} + \frac{\partial^2\eta}{\partial\tau^2} + c\frac{\partial\eta}{\partial\tau} + k_{\mathrm{w}}\eta - q(\xi,\tau)\right] = 0
\end{aligned} \tag{5}$$

For pinned–pinned (P–P) boundary condition at $\xi = 0, 1$

$$\eta = 0,$$

$$\begin{aligned}
&-\left(1+\alpha\frac{\partial}{\partial\tau}\right)\frac{\partial^2\eta}{\partial\xi^2} + \mu^2\left[\left((\mathrm{VCF}\times u)^2 - N - k_{\mathrm{G}}\right)\frac{\partial^2\eta}{\partial\xi^2}\right.\\
&\left. + 2(\mathrm{VCF}\times u)\sqrt{\beta}\frac{\partial^2\eta}{\partial\xi\partial\tau} + \frac{\partial^2\eta}{\partial\tau^2} + c\frac{\partial\eta}{\partial\tau} + k_{\mathrm{w}}\eta - q(\xi,\tau)\right] = 0
\end{aligned} \tag{6}$$

For clamped–pinned (C–P) boundary condition at $\xi = 0$

$$\eta = \frac{\partial\eta}{\partial\xi} = 0$$

at $\xi = 1$

$$\eta = 0,$$

$$-\left(1+\alpha\frac{\partial}{\partial\tau}\right)\frac{\partial^2\eta}{\partial\xi^2}+\mu^2\left[\left((\mathrm{VCF}\times u)^2-N-k_{\mathrm{G}}\right)\frac{\partial^2\eta}{\partial\xi^2}+2(\mathrm{VCF}\times u)\sqrt{\beta}\frac{\partial^2\eta}{\partial\xi\partial\tau}+\frac{\partial^2\eta}{\partial\tau^2}+c\frac{\partial\eta}{\partial\tau}+k_{\mathrm{w}}\eta-q(\xi,\tau)\right]=0$$

For clamped–clamped (C–C) boundary condition at $\xi = 0, 1$

$$\eta=\frac{\partial\eta}{\partial\xi}=0$$

Let us define harmonic concentrate force, q, as:

$$q(\xi,\tau)=F_0\delta(\xi-l)e^{\omega\tau i} \tag{7}$$

where $\delta(\cdot)$ is the Dirac delta function, ω is the excitation frequency and ℓ is non-dimensional position of the concentrated force.

3 Application of GFM to solve the forced vibration of CNT conveying fluid

Different analytical techniques can be implemented to solve the governing equation and related boundary conditions. Among them, the GFM has revealed a great potential in solving complicated partial differential equations and has been successfully applied in many examinations. In current study, the size-dependent thermomechanical dynamic deflection of CNTs conveying fluid resting on visco-Pasternak medium with different boundary conditions is studied using analytical GFM. Thus, the results obtained by the present solution are accurate than those in previous results. In order to eliminate time variable from Eq. (5), substitute the expression $\eta(\xi,\tau)=X(\xi)e^{\omega\tau i}$ and Eq. (7) into Eq. (5). Consequently, the steady-state vibration equation of CNT conveying fluid is recasted to

$$\lambda_1\frac{\partial^4X(\xi)}{\partial\xi^4}+\lambda_2\frac{\partial^3X(\xi)}{\partial\xi^3}+\lambda_3\frac{\partial^2X(\xi)}{\partial\xi^2}+\lambda_4\frac{\partial X(\xi)}{\partial\xi}+\lambda_5X(\xi)=\left(1-\mu^2\frac{\partial^2}{\partial\xi^2}\right)f(\xi) \tag{8}$$

where

$$\begin{aligned}
\lambda_1&=1+\omega\alpha i-\mu^2\left((\mathrm{VCF}-u)^2-N-k_{\mathrm{G}}\right)\\
\lambda_2&=-2\omega\mu^2(\mathrm{VCF}\times u)\sqrt{\beta}i\\
\lambda_3&=(\mathrm{VCF}\times u)^2-N-k_{\mathrm{G}}-\mu^2\left(k_{\mathrm{w}}+\omega ci-\omega^2\right)\\
\lambda_4&=2\omega(\mathrm{VCF}\times u)\sqrt{\beta}i\\
\lambda_5&=k_{\mathrm{w}}+\omega ci-\omega^2
\end{aligned} \tag{9}$$

According to superposition principle, the solution of Eq. (8) can be written in the following form (Nicholson and Bergman 1986):

$$X(\xi)=\int_0^1 f\left(\xi_0\right)G\left(\xi,\xi_0\right)\mathrm{d}\xi_0 \tag{10}$$

where $G(\xi, \xi_0)$ denotes the Green's function. Physically, a Green's function of the steady-state vibration equation of the beam is the deflection of its steady-state response due to a unit concentrated harmonic stimulus acting at an arbitrary position. Therefore, to obtain the Green function, we first consider $f(\xi) = \delta(\xi - \xi_0)$ in Eq. (8) and then take Laplace transform on both sides of the equation in terms of the variable ξ which lead to the following equation:

$$\begin{aligned}
\bar{X}\left(s,\xi_0\right)&=\frac{1}{\Lambda_1}\left[\left(1-\mu^2s^2\right)e^{-s\xi_0}+\Lambda_2X(0)+\Lambda_3X'(0)+\Lambda_4X''(0)+\lambda_1X'''(0)\right],\\
\Lambda_1&=\lambda_1s^4+\lambda_2s^3+\lambda_3s^2+\lambda_4s+\lambda_5\\
\Lambda_2&=\lambda_1s^3+\lambda_2s^2+\lambda_3s+\lambda_4\\
\Lambda_3&=\lambda_1s^2+\lambda_2s+\lambda_3\\
\Lambda_4&=\lambda_1s+\lambda_2
\end{aligned} \tag{11}$$

where s is a complex Laplace variable and $\bar{X}\left(s,\xi_0\right)$ is Laplace transform of $X(s, \xi_0)$; further, $X(0)$, $X'(0)$, $X''(0)$ and $X'''(0)$ are constants to be determined from the boundary conditions. To obtain Green function, by performing the inverse Laplace transform of Eq. (11), we arrive at

$$\begin{aligned}
G\left(\xi,\xi_0\right)&=X\left(\xi,\xi_0\right)=L^{-1}\left[\bar{X}\left(s,\xi_0\right)\right]\\
&=\phi_1(\xi)X(0)+\phi_2(\xi)X'(0)\\
&\quad+\phi_3(\xi)X''(0)+\lambda_1\phi_4(\xi)X'''(0)\\
&\quad+\phi_4\left(\xi-\xi_0\right)H\left(\xi-\xi_0\right)\\
&\quad-\mu^2\phi_5\left(\xi-\xi_0\right)H\left(\xi-\xi_0\right)
\end{aligned} \tag{12}$$

where $H(\cdot)$ is the Heaviside function and $\phi_i(\xi)$ (i = 1, 2, …, 5) are

$$\begin{aligned}
\phi_1(\zeta)&=\sum_{i=1}^4R_i(\zeta)\left(\lambda_1s_i^3+\lambda_2s_i^2+\lambda_3s_i+\lambda_4\right),\\
\phi_2(\zeta)&=\sum_{i=1}^4R_i(\zeta)\left(\lambda_1s_i^2+\lambda_2s_i+\lambda_3\right),\\
\phi_3(\zeta)&=\sum_{i=1}^4R_i(\zeta)\left(\lambda_1s_i+\lambda_2\right),\\
\phi_4(\zeta)&=\sum_{i=1}^4R_i(\zeta),\quad \phi_5(\zeta)=\sum_{i=1}^4R_i(\zeta)s_i^2
\end{aligned} \tag{13}$$

with

$$R_1(\zeta) = \frac{e^{s_1\zeta}}{(s_1 - s_2)(s_1 - s_3)(s_1 - s_4)},$$
$$R_2(\zeta) = \frac{e^{s_2\zeta}}{(s_2 - s_1)(s_2 - s_3)(s_2 - s_4)},$$
$$R_3(\zeta) = \frac{e^{s_3\zeta}}{(s_3 - s_1)(s_3 - s_2)(s_3 - s_4)}, \tag{14}$$
$$R_4(\zeta) = \frac{e^{s_4\zeta}}{(s_4 - s_1)(s_4 - s_2)(s_4 - s_3)}.$$

Also, s_i ($i = 1, \ldots, 4$) are roots of the left-hand term of equation $\Lambda_1 = 0$. The first, second and third derivatives of $X(\xi, \xi_0)$ in terms of ξ for $\xi \geq \xi_0$ are given by:

$$X'(\xi,\xi_0) = \phi_1'(\xi)X(0) + \phi_2'(\xi)X'(0) + \phi_3'(\xi)X''(0) + \lambda_1\phi_4'(\xi)X'''(0) + \phi_4'(\xi-\xi_0)H(\xi-\xi_0) - \mu^2\phi_5'(\xi-\xi_0)H(\xi-\xi_0) \tag{15}$$

$$X''(\xi,\xi_0) = \phi_1''(\xi)X(0) + \phi_2''(\xi)X'(0) + \phi_3''(\xi)X''(0) + \lambda_1\phi_4''(\xi)X'''(0) + \phi_4''(\xi-\xi_0)H(\xi-\xi_0) - \mu^2\phi_5''(\xi-\xi_0)H(\xi-\xi_0) \tag{16}$$

$$\begin{aligned} X'''(\xi,\xi_0) = {} & \phi_1'''(\xi)X(0) + \phi_2'''(\xi)X'(0) \\ & + \phi_3'''(\xi)X''(0) + \lambda_1\phi_4'''(\xi)X'''(0) \\ & + \phi_4'''(\xi-\xi_0)H(\xi-\xi_0) \\ & - \mu^2\phi_5'''(\xi-\xi_0)H(\xi-\xi_0) \end{aligned} \tag{17}$$

Inserting $\xi = 1$ into Eqs. (12), (15–17) and substituting them into boundary conditions where it is needed and with further manipulations, the following relation in matrix form can be expressed as:

$$\begin{bmatrix} A_{11} & A_{12} & A_{13} & A_{14} \\ A_{21} & A_{22} & A_{23} & A_{24} \\ A_{31} & A_{32} & A_{33} & A_{34} \\ A_{41} & A_{42} & A_{43} & A_{44} \end{bmatrix} \begin{bmatrix} X(0) \\ X'(0) \\ X''(0) \\ X'''(0) \end{bmatrix} = \begin{bmatrix} B_{11} \\ B_{21} \\ B_{31} \\ B_{41} \end{bmatrix} \tag{18}$$

For fluid-conveying CNT, "Appendix 2" lists the coefficient matrix elements A_{ij} and B_{ij} from which the constants $X(0)$, $X'(0)$, $X''(0)$ and $X'''(0)$ can be determined completely for each boundary conditions. Then, by substituting these constants into Eq. (12) the Green function is determined. Thus, inserting Green function and $f(\xi_0) = F_0\delta(\xi_0 - \ell)$ into Eq. (10) yields the following equation

$$\begin{aligned} X(\xi) = {} & \int_0^1 F_0\delta(\xi_0 - \ell)\left[\phi_1(\xi)X(0) + \phi_2(\xi)X'(0) + \phi_3(\xi)X''(0) + \lambda_1\phi_4(\xi)X'''(0)\right]\mathrm{d}\xi_0 \\ & + \int_0^1 F_0\delta(\xi_0 - \ell)\left[\phi_4(\xi-\xi_0)H(\xi-\xi_0) - \mu^2\phi_5(\xi-\xi_0)H(\xi-\xi_0)\right]\mathrm{d}\xi_0 \end{aligned} \tag{19}$$

The relation of delta function can be expressed as:

$$\int_{\alpha_0}^{\beta_0} \phi_i(\xi)\delta(\xi-\xi_0)\mathrm{d}\xi = \begin{cases} 0 & \xi_0 < \alpha_0 \\ \phi_i(\xi_0) & \alpha_0 < \xi_0 < \beta_0 \\ 0 & \xi_0 > \beta_0 \end{cases} \tag{20}$$

Therefore, the first and second integrations are given by:

$$\begin{aligned} I_1(\xi) = F_0\Big\{ & \phi_1(\xi)[X(0)]_{\xi_0=\ell} + \phi_2(\xi)\left[X'(0)\right]_{\xi_0=\ell} \\ & + \phi_3(\xi)\left[X''(0)\right]_{\xi_0=\ell} + \lambda_1\phi_4(\xi)\left[X'''(0)\right]_{\xi_0=\ell}\Big\} \end{aligned} \tag{21a}$$

$$I_2(\xi) = \begin{cases} 0 & 0 < \xi < l \\ F_0\left\{\phi_4(\xi-\ell) - \mu^2\phi_5(\xi-\ell)\right\} & l < \xi < 1 \end{cases} \tag{21b}$$

Thus, the dynamic response of the CNT conveying fluid is written as:

$$X(\xi) = I_1(\xi) + I_2(\xi) \tag{22}$$

The dynamic response obtained from Eq. (22) is in general complex. Therefore, the real form of dynamic response of the CNT conveying fluid can be written as:

$$\eta(\xi,\tau) = Re[X(\xi)]\cos(\omega\tau) - Im[X(\xi)]\sin(\omega\tau) \tag{23}$$

4 Results and discussion

In all numerical calculations in this section, it was assumed that CNT carries a harmonic concentrated force at the mid-span ($\ell = 0.5$). In order to justify the validity of the present analysis, the natural frequency and maximum deflection of CNT conveying fluid obtained by the present solution are compared with those in previous results. For this purpose, Fig. 2 depicts the variation of maximum dynamic deflection for the pinned–pinned CNT versus excitation frequency. It can be seen that with increase in excitation frequency, the maximum dynamic deflection of the system first increases and then tends to decrease. Also, the excitation frequency at which the maximum dynamic deflection is reached is related to the natural frequency. Therefore, the achieved first four dimensionless natural frequencies which are obtained by this method are compared with those reported by Wang et al. (2007) and good agreement is observed. The calculation of maximum dynamic deflection for clamped–clamped boundary conditions is similar to that for P–P boundary condition, but not shown here. Also, the results of natural frequencies are tabulated in Table 1. It should be mentioned that to compare the results with those proposed by Wang et al. (2007), the effects of the Knudsen number, temperature change and visco-Pasternak foundation are assumed to be neglected. Moreover, the natural frequencies predicted by using the nonlocal theory ($\mu \neq 0$) are always lower than

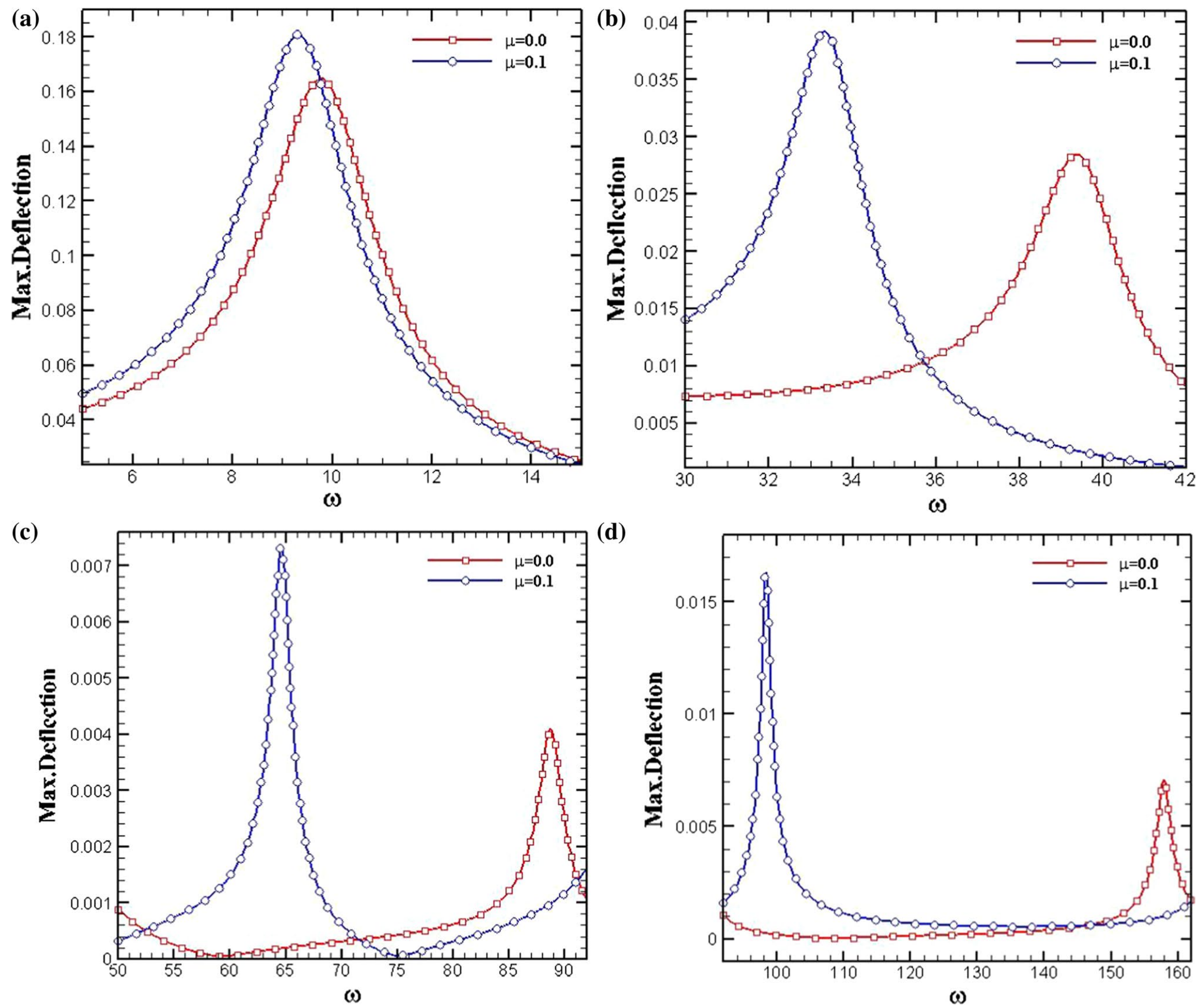

Fig. 2 Dimensionless maximum dynamic deflection of pinned–pinned CNT versus dimensionless excitation frequency for $\alpha = 0$, $\Delta T = 0$, $u = 0$, $\beta = 0.5$, $Kn = 0$, $F = 2$, $\xi = 0.3$, $k_w = 0$, $k_G = 0$, $c = 2$: **a** near ω_1, **b** near ω_2, **c** near ω_3, **d** near ω_4

Table 1 Comparison of the four first frequency parameters $\sqrt{\omega}$ obtained from the present model with the results reported by Wang et al. (2007) for $\alpha = 0$, $\Delta T = 0$, $u = 0$, $\beta = 0.5$, $Kn = 0$, $F = 2$, $k_w = 0$, $k_G = 0$, $c = 2$

Boundary conditions	Pinned–pinned				Clamed-pinned			
Research	Wang et al. (2007)		Present study		Wang et al. (2007)		Present study	
Nonlocal parameter	$\mu = 0$	$\mu = 0.1$	$\mu = 0$	$\mu = 0.1$	$\mu = 0$	$\mu = 0.1$	$\mu = 0$	$\mu = 0.1$
1st frequency	3.1416	3.0685	3.1384	3.0512	3.9266	3.8209	3.9266	3.8209
2nd frequency	6.2832	5.5304	6.2327	5.4561	7.0686	6.4649	7.0654	6.4621
3rd frequency	9.4248	7.4699	9.4127	7.3543	10.2102	8.6517	10.1965	8.6504
4th frequency	12.5660	8.9874	12.5432	8.8798	13.3518	10.4690	13.3501	10.4651

those obtained by the classical theory ($\mu = 0$). This means that the effect of nonlocal parameter softens the CNTs and consequently causes to increase in maximum dynamic deflections. Furthermore, the comparison of the maximum dynamic deflections of CNT without considering the nonlocal effect, Knudsen number and viscoelastic Pasternak medium is presented in Table 2, for different values of fluid velocities against results presented by Li and Yang (2014). It is observed from Table 2 that the current model is actually in good agreement with previous models. After

Table 2 Comparison of the maximum deflections obtained from the present study with the results obtained by Li and Yang (2014) for a clamped–clamped pipe conveying fluid at position $\xi = 0.8536$

Flow velocity	Present study	Li and Yang (2014)	
	GFM	GFM	Galerkin method
0.0	0.002744	0.002744	0.002943
4.0	0.005778	0.005778	0.006213
5.0	0.017043	0.017043	0.016924
6.0	0.011018	0.011018	0.015108

this verification, it was discussed on the numerical results concerned with the forced vibration response of viscoelastic CNTs conveying fluid subjected to thermal field and resting on visco-Pasternak foundation with various boundary conditions. Therefore, this section assigned to show the effects of nonlocal parameter, fluid velocity, visco-Pasternak foundation, Knudsen number, structural damping of CNT, temperature change and various boundary conditions on the dynamic deflections of CNT in several numerical examples. In this regard, the values for several physical parameters of the system are with the following data (Ávila and Lacerda 2008; Mirramezani and Mirdamadi 2012; Yakobson et al. 1996; Yao and Han 2008):

$$E = 5.5\ \text{TPa}, \quad \nu = 0.2, \quad \rho_{\text{CNT}} = 2300\,\text{kg/m}^3,$$
$$\rho_{\text{f}} = 790\,\text{kg/m}^3, \quad 2R_{\text{o}} = 1\,\text{nm},$$
$$h = 0.066\,\text{nm}, \quad L/2R_{\text{o}} = 10$$

On the basis of the reported results by Sazonova et al. (2004), the viscoelastic structural damping coefficient (g) may vary from 0 to 1.45×10^{-11} s for the problem under

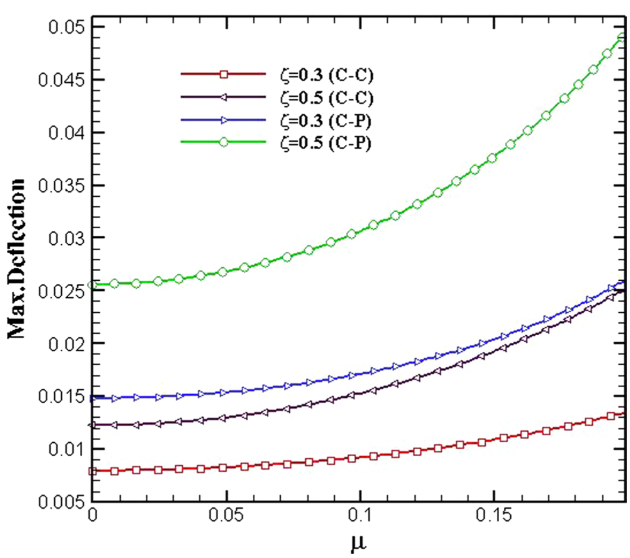

Fig. 3 Effects of the boundary conditions on the dimensionless maximum dynamic deflection versus dimensionless nonlocal parameter for $\alpha = 0$, $\Delta T = 0$, $\beta = 0.5$, $Kn = 0.01$, $\omega = 4$, $F = 2$, $u = 2$, $k_{\text{w}} = 0$, $k_{\text{G}} = 0$, $c = 0$

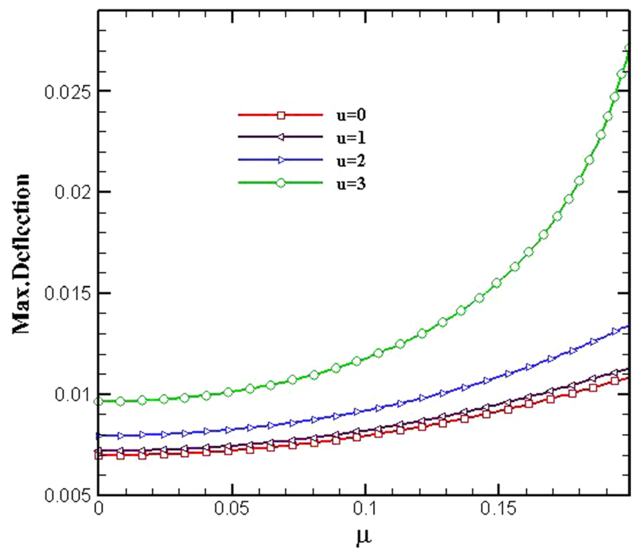

Fig. 4 Effects of the fluid velocities on the dimensionless maximum dynamic deflection versus dimensionless nonlocal parameter for $\alpha = 0$, $\Delta T = 0$, $\beta = 0.5$, $Kn = 0.01$, $\omega = 4$, $F = 2$, $\xi = 0.3$, $k_{\text{w}} = 0$, $k_{\text{G}} = 0$, $c = 0$ and clamped–clamped boundary conditions

investigation. So, we will use a conservative range of dimensionless viscoelastic damping coefficient α from 0 to 1. Also, in this paper, the nonlocal and material length scale parameter e_0a will vary from 0 to 2 nm (μ = 0–0.2).

Figures 3 and 4 illustrate the dimensionless maximum dynamic deflection versus nonlocal parameter for different boundary conditions and various values of fluid velocities, respectively. Figure 3 reveals that by increasing the value of nonlocal parameter, the dimensionless maximum dynamic deflection of CNT conveying fluid increases. In other words, with the increase in nonlocal parameter, the CNT stiffness decreases and dimensionless maximum dynamic deflection increases. Figure 4 shows that by increasing the value of fluid velocity, the dimensionless maximum dynamic deflection of clamped–clamped CNT conveying fluid increases.

The structural damping coefficient of CNT on the dimensionless maximum dynamic deflection of a clamped-pinned CNT conveying fluid is studied as shown in Fig. 5. As seen in these figures, by increasing the structural damping coefficient, the dimensionless maximum dynamic deflection of the system decreases. In Fig. 5a, b, the influences of nonlocal parameter and mass ratio on the variation of dimensionless maximum dynamic deflection versus structural damping coefficient of CNT are shown. With the increase in nonlocal parameter and mass ratio, dimensionless maximum dynamic deflection decreases. As shown in Fig. 5c, by increasing the fluid velocity, the dimensionless maximum dynamic deflection increases. It can be seen that for $\alpha > 0.8$, the fluid velocity has not more significant effect on dimensionless maximum dynamic deflection.

Figure 6 indicates effect of elastic foundation, including Winkler, Pasternak and visco-Pasternak

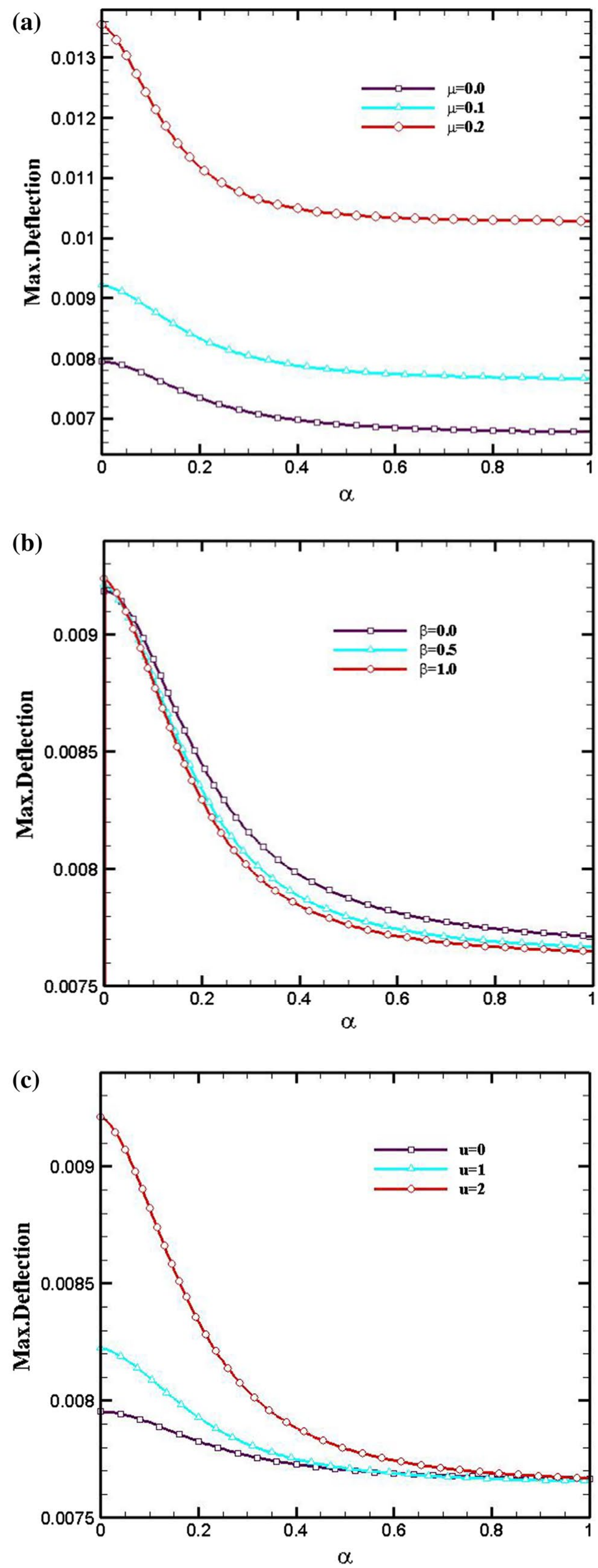

Fig. 5 Maximum dimensionless dynamic deflection in terms of structural damping coefficient of clamped-pinned CNT for $\Delta T = 0$, $Kn = 0.01$, $\omega = 4$, $F = 2$, $\xi = 0.3$, $k_{\mathrm{w}} = 0$, $k_{\mathrm{G}} = 0$, $c = 0$ and different values of: **a** μ ($\beta = 0.5$ and $u = 2$), **b** β ($\mu = 0.1$ and $u = 2$), **c** u ($\mu = 0.1$ and $\beta = 0.5$)

mediums on dimensionless maximum dynamic deflection of clamped–clamped CNT as a function of ξ. It is seen that dimensionless maximum dynamic deflection is dependent on the spring, shear and damping modulus of the surrounding foundation. Also, it is observed from the figure that the dimensionless maximum dynamic deflection predicted by visco-Pasternak foundation is smaller than that predicted by Winkler foundation, and it is due to the more elastic foundation stiffness that predicted in visco-Pasternak medium model in comparison with other models.

Effect of the temperature change on dimensionless maximum dynamic deflection of the clamped–clamped CNT conveying fluid is presented in Fig. 7. The results are shown in two coefficients of thermal expansion corresponding to room or low temperature ($\alpha_x = -1.6 \times 10^{-6}$1/K) and high temperature ($\alpha_x = 1.1 \times 10^{-6}$1/K). For the case of room or low temperature, the dimensionless maximum dynamic deflection decreases with increasing the temperature change, whereas resonance frequency of forced vibration shifts rightwards. For the case of high temperature, it is observed that the dimensionless maximum dynamic deflection incorporating thermal effect is larger than those excluding the influence of temperature change. Indeed, increase in temperature change of the negative/positive coefficients of thermal expansion increases/decreases the stiffness and natural frequency of the CNT conveying fluid.

Figure 8 indicates the influences of Knudsen number on the variation of dimensionless maximum dynamic deflection in terms of excitation frequency for the case of low temperature. It can be observed that by increasing the Knudsen number, which is the ratio of mean free path of the fluid molecules to the length of flow property, the dimensionless maximum dynamic deflection increases, whereas the natural frequency of clamped–clamped CNT conveying fluid reduces. As shown, at low excitation frequencies away from the natural frequency the increase in Kn causes an increase in maximum dynamic deflection, but as the excitation frequency increases the opposite behavior is observed. Furthermore, by increasing Kn from 0 to 0.01 there is no noticeable change in maximum dynamic deflection.

Figure 9 shows the dimensionless maximum dynamic deflection versus excitation frequency for the case of low temperature and different boundary conditions. As expected, pinned–pinned CNT has a bigger maximum dynamic deflection than clamped–clamped CNT, whereas structural stiffness of clamped–clamped CNT conveying fluid is higher than other boundary conditions.

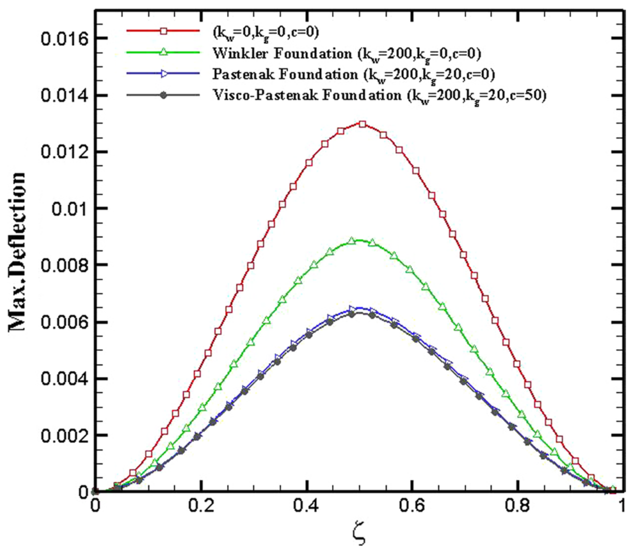

Fig. 6 Effects of the elastic foundation on the dimensionless maximum dynamic deflection versus dimensionless ξ for $\alpha = 0.001$, $\Delta T = 0$, $\beta = 0.5$, $\mu = 0.05$, $Kn = 0.01$, $\omega = 4$, $F = 2$ and clamped–clamped boundary conditions

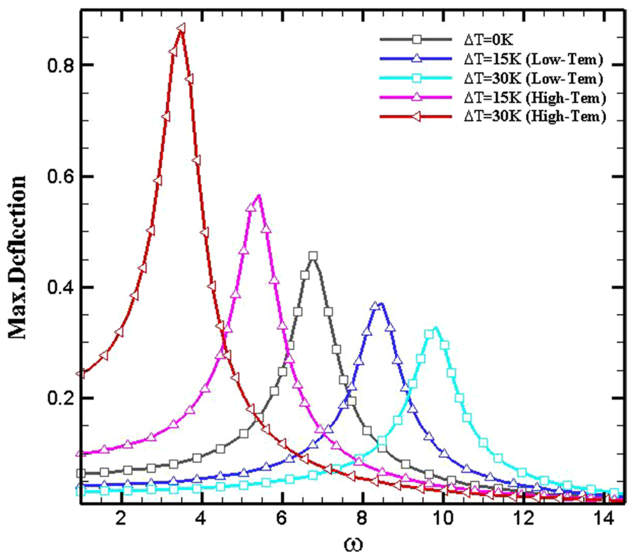

Fig. 7 Effects of the temperature changes on the dimensionless maximum dynamic deflection versus dimensionless excitation frequency for $\alpha = 0.001$, $\beta = 0.5$, $\mu = 0.1$, $Kn = 0$, $\omega = 4$, $F = 2$, $\xi = 0.3$, $k_w = 0$, $k_G = 0$, $c = 0$ and clamped–clamped boundary conditions

5 Conclusions

This research addressed the flow-thermoelastic forced vibration of viscoelastic CNT resting on visco-Pasternak foundation and subjected to various boundary conditions. To consider the slip boundary condition between the wall of CNT and fluid, the Knudsen-dependent flow velocity is employed. Due to incapability of classical elasticity theory to demonstration the small-scale effects, Eringen's nonlocal theory was employed to

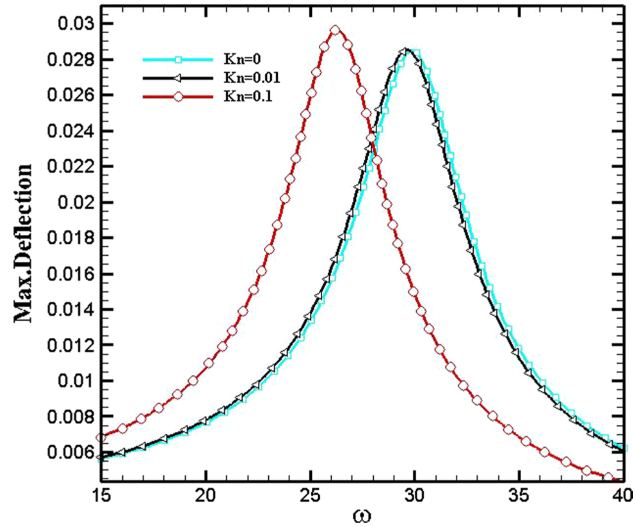

Fig. 8 Effects of the Knudsen number on the dimensionless maximum dynamic deflection versus dimensionless excitation frequency for $\alpha = 0.001$, $\Delta T = 15$ (low temperature), $\beta = 0.5$, $\mu = 0.1$, $\omega = 4$, $F = 2$, $\xi = 0.3$, $k_w = 200$, $k_G = 20$, $c = 5$ and clamped–clamped boundary conditions

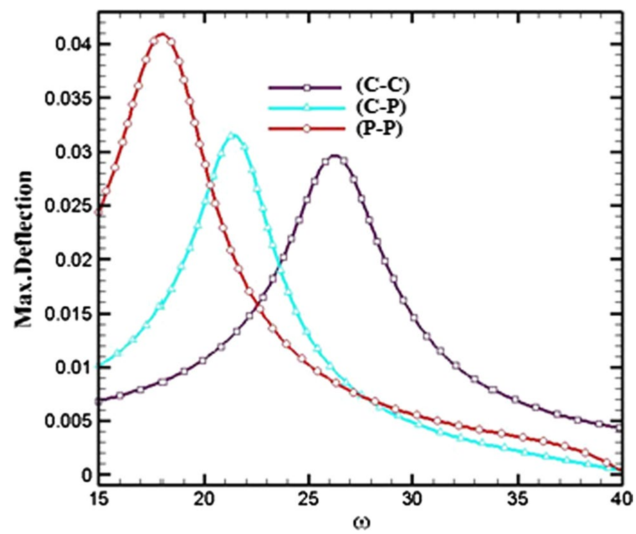

Fig. 9 Effects of the boundary conditions on the dimensionless maximum dynamic deflection versus dimensionless excitation frequency for $\alpha = 0.001$, $\Delta T = 15$ (low temperature), $\beta = 0.5$, $\mu = 0.1$, $Kn = 0.1$, $\omega = 4$, $F = 2$, $\xi = 0.3$, $k_w = 200$, $k_G = 20$, $c = 5$

capture the size effects. The GFM was implemented for solving the governing differential equation to achieve the dynamic deflections of CNTs. It was found that the increase in nonlocal parameters leads to increasing non-dimension maximum dynamic deflections of CNTs conveying fluid. Furthermore, it was seen that by the increase in structural damping coefficient of CNT, the dimensionless maximum dynamic deflections decrease. In addition, it was shown that the temperature change has significant effect on the dimensionless maximum dynamic deflections of CNTs. Moreover, the results indicated that dimensionless maximum dynamic deflection of visco-Pasternak and Winkler mediums is minimum and maximum, respectively, while Pasternak type is between of them.

Appendix 1

Viscosity in nanoflows

For the effective viscosity of fluid in terms of Kn number, relation between effective viscosity μ_e and bulk viscosity μ_0 is formulated as (Beskok and Karniadakis 1999):

$$\mu_e = \mu_0\left(\frac{1}{1+\bar{a}Kn}\right) \tag{24}$$

where $\bar{a}$ is a coefficient which is dependent to Knudsen number, as follows (Karniadakis et al. 2005):

$$\bar{a} = a_0\frac{2}{\pi}\left[\tan^{-1}\left(a_1 Kn^B\right)\right] \tag{25}$$

here $a_1 = 4$ and $B = 0.4$ represent empirical parameters and a_0 is defined as (Karniadakis et al. 2005):

$$\lim_{Kn\to\infty}\bar{a} = a_0 = \frac{64}{3\pi\left(1-\frac{4}{b}\right)} \tag{26}$$

where b represent a general slip coefficient. By choosing $b = -1$, we reach a second-order term of slip boundary condition equation.

Slip boundary conditions

The slip velocity model to consider the slip boundary conditions in nanoflow field as (Beskok and Karniadakis 1999)

$$V_s - V_w = \left(\frac{2-\sigma_v}{\sigma_v}\right)\left(\frac{Kn}{1-bKn}\right)\left(\frac{\partial v_x}{\partial n}\right) \tag{27}$$

where V_s, V_w and σ_v are slip velocity of the flow near nanotube's wall, axial velocity of wall velocity and tangential moment accommodation coefficient, respectively. Furthermore, v_x denote the axial flow velocity, n is the normal vector, and σ_v is expressed as below (Beskok and Karniadakis 1999):

$$\sigma_v = \frac{\left(\tau_i - \tau_r\right)}{\left(\tau_i - \tau_w\right)} \tag{28}$$

where τ_i, τ_r and τ_w denote, respectively, tangential momentum of incoming, reflected and reemitted molecules. The value of σ_v is equal to 0.7 (Shokouhmand et al. 2010).

Derivation of the average velocity correction factor

For investigating the effect of flow passing through a CNT, we consider a homogeneous fluid, isothermal isotropic, fully developed laminar, incompressible, parallel and viscous fluid flow of constant density and viscosity. For a Newtonian fluid, considering a constant pressure gradient along CNT length, and neglecting the effects of gravitational and electromagnetic body forces, the well-known Navier–Stokes equations are stated as follows (Shames and Shames 1982)

$$\rho\frac{d\vec{V}}{dt} = -\vec{\nabla}P + \mu_e\nabla^2\vec{V} \tag{29}$$

where ρ, V and P are the fluid density, flow velocity vector and pressure, respectively. By these assumptions, the fluid velocity distribution by solving Navier–Stokes equation can be expressed as (Shames and Shames 1982)

$$v_x = \frac{1}{4\mu_e}\left(\frac{\partial P}{\partial x}\right)r^2 + C_3\ln(r) + C_4 \tag{30}$$

where r and x, respectively, represent the CNT radius and longitudinal coordinate of CNT elastic axis and axial flow. The boundary conditions enforce $C_3 = 0$. In order to obtain C_4, the slip boundary conditions at the CNT wall can be applied:

$$v_{x(r=R_i)} = R_i\left(\frac{2-\sigma_v}{\sigma_v}\right)\left(\frac{Kn}{1-bKn}\right)\left(\frac{\partial v_x}{\partial r}\right)_{r=R_i} \tag{31}$$

where R_i denote the inner radius of the CNT. Thus, Eq. (30) may be written as:

$$V_{slip}(r) = \frac{1}{4\mu_0\left(\frac{1}{1+aKn}\right)}\left(\frac{\partial P}{\partial x}\right)\left[r^2 - R^2 - 2R^2\left(\frac{2-\sigma_v}{\sigma_v}\right)\left(\frac{Kn}{1+Kn}\right)\right] \tag{32}$$

Therefore, the average fluid velocities through nanotube with slip boundary conditions can be obtained as:

$$\begin{aligned} U_{ave,\,slip} &= \frac{1}{A}\int_A V_{slip}(r)\mathrm{d}A = \frac{2}{R^2}\int_0^{R_i} V_{slip}(r)r\mathrm{d}r \\ &= \frac{R^2}{8\mu_0\left(\frac{1}{1+aKn}\right)}\left(-\frac{\partial P}{\partial x}\right)\left(4\left(\frac{2-\sigma_v}{\sigma_v}\right)\left(\frac{Kn}{1+Kn}\right)+1\right) \end{aligned} \tag{33}$$

For no-slip boundary conditions, the Kn approaches to zero in Eqs. (32, 33). Finally, the dimensionless average velocity correction is represented as:

$$\mathrm{VCF} \equiv \frac{U_{avg,slip}}{U_{avg,(no\text{ - }slip)}} = (1+aKn)\left[4\left(\frac{2-\sigma_v}{\sigma_v}\right)\left(\frac{Kn}{1+Kn}\right)+1\right] \tag{34}$$

where $U_{avg,slip}$ and $U_{avg,(no\text{-}slip)}$ are the average fluid velocities through nanotube with slip boundary conditions and without slip boundary conditions, respectively. With considering the average velocity correction factor, the flow velocity can be expressed as $U_{avg,slip} = \mathrm{VCF}\times U_{avg,(no\text{-}slip)}$.

Appendix 2

The coefficient matrix elements A_{ij} and B_{ij} are derived for various boundary conditions.

- For P–P boundary condition

Symbol	Value	Symbol	Value
A_{11}	1	A_{31}	$\phi_1(1)$
A_{12}	0	A_{32}	$\phi_2(1)$
A_{13}	0	A_{33}	$\phi_3(1)$
A_{14}	0	A_{34}	$\lambda_1\phi_4(1)$
A_{21}	$\mu^2\lambda_5$	A_{41}	$-\lambda_1\phi_1''(1)-\lambda_2\phi_1'(1)+\mu^2\lambda_5\phi_1(1)$
A_{22}	$-\lambda_2$	A_{42}	$-\lambda_1\phi_2''(1)-\lambda_2\phi_2'(1)+\mu^2\lambda_5\phi_2(1)$
A_{23}	$-\lambda_1$	A_{43}	$-\lambda_1\phi_3''(1)-\lambda_2\phi_3'(1)+\mu^2\lambda_5\phi_3(1)$
A_{24}	0	A_{44}	$-\lambda_1^2\phi_4''(1)-\lambda_2\lambda_1\phi_4'(1)+\mu^2\lambda_5\lambda_1\phi_4(1)$
B_{11}	0	B_{31}	$\mu^2\phi_5(1-\xi_0)H(1-\xi_0)-\phi_4(1-\xi_0)H(1-\xi_0)$
B_{21}	0	B_{41}	$\lambda_1[\phi_4''(1-\xi_0)H(1-\xi_0)-\mu^2\phi_5''(1-\xi_0)H(1-\xi_0)]+\lambda_2[\phi_4'(1-\xi_0)$ $H(1-\xi_0)-\mu^2\phi_5'(1-\xi_0)H(1-\xi_0)]-\mu^2\lambda_5[\phi_4(1-\xi_0)H(1-\xi_0)-$ $\mu^2\phi_5(1-\xi_0)H(1-\xi_0)]$

- For C–P boundary condition

Symbol	Value	Symbol	Value
A_{11}	1	A_{31}	$\phi_1(1)$
A_{12}	0	A_{32}	$\phi_2(1)$
A_{13}	0	A_{33}	$\phi_3(1)$
A_{14}	0	A_{34}	$\lambda_1\phi_4(1)$
A_{21}	0	A_{41}	$-\lambda_1\phi_1''(1)-\lambda_2\phi_1'(1)+\mu^2\lambda_5\phi_1(1)$
A_{22}	1	A_{42}	$-\lambda_1\phi_2''(1)-\lambda_2\phi_2'(1)+\mu^2\lambda_5\phi_2(1)$
A_{23}	0	A_{43}	$-\lambda_1\phi_3''(1)-\lambda_2\phi_3'(1)+\mu^2\lambda_5\phi_3(1)$
A_{24}	0	A_{44}	$-\lambda_1^2\phi_4''(1)-\lambda_2\lambda_1\phi_4'(1)+\mu^2\lambda_5\lambda_1\phi_4(1)$
B_{11}	0	B_{31}	$\mu^2\phi_5(1-\xi_0)H(1-\xi_0)-\phi_4(1-\xi_0)H(1-\xi_0)$
B_{21}	0	B_{41}	$\lambda_1[\phi_4''(1-\xi_0)H(1-\xi_0)-\mu^2\phi_5''(1-\xi_0)H(1-\xi_0)]+\lambda_2[\phi_4'(1-\xi_0)H(1-\xi_0)-\mu^2\phi_5'(1$ $-\xi_0)H(1-\xi_0)]-\mu^2\lambda_5[\phi_4(1-\xi_0)H(1-\xi_0)-\mu^2\phi_5(1-\xi_0)H(1-\xi_0)]$

- For C–C boundary condition

Symbol	Value	Symbol	Value
A_{11}	1	A_{31}	$\phi_1(1)$
A_{12}	0	A_{32}	$\phi_2(1)$
A_{13}	0	A_{33}	$\phi_3(1)$
A_{14}	0	A_{34}	$\lambda_1\phi_4(1)$
A_{21}	0	A_{41}	$\phi_1'(1)$
A_{22}	1	A_{42}	$\phi_2'(1)$
A_{23}	0	A_{43}	$\phi_3'(1)$
A_{24}	0	A_{44}	$\lambda_1\phi_4'(1)$
B_{11}	0	B_{31}	$\mu^2\phi_5(1-\xi_0)H(1-\xi_0)-\phi_4(1-\xi_0)H(1-\xi_0)$
B_{21}	0	B_{41}	$\mu^2\phi_5'(1-\xi_0)H(1-\xi_0)-\phi_4'(1-\xi_0)H(1-\xi_0)$

References

Ansari R, Sahmani S (2012) Small scale effect on vibrational response of single-walled carbon nanotubes with different boundary conditions based on nonlocal beam models. Commun Nonlinear Sci Numer Simul 17:1965–1979

Ansari R, Norouzzadeh A, Gholami R, Faghih Shojaei M, Darabi MA (2016) Geometrically nonlinear free vibration and instability of fluid-conveying nanoscale pipes including surface stress effects. Microfluid Nanofluid 20:28. https://doi.org/10.1007/s10404-015-1669-y

Arani AG, Amir S (2013) Electro-thermal vibration of visco-elastically coupled BNNT systems conveying fluid embedded on elastic foundation via strain gradient theory. Physica B 419:1–6

Askari H, Esmailzadeh E (2017) Forced vibration of fluid conveying carbon nanotubes considering thermal effect and nonlinear foundations. Compos B Eng 113:31–43. https://doi.org/10.1016/j.compositesb.2016.12.046

Askari H, Zhang D, Esmailzadeh E (2013) Nonlinear vibration of fluid-conveying carbon nanotube using homotopy analysis method. In: 2013 13th IEEE international conference on nanotechnology (IEEE-NANO 2013), 5–8 August 2013, pp 545–548. https://doi.org/10.1109/NANO.2013.6720962

Ávila AF, Lacerda GSR (2008) Molecular mechanics applied to single-walled carbon nanotubes. Mater Res 11:325–333

Bahaadini R, Hosseini M (2016a) Effects of nonlocal elasticity and slip condition on vibration and stability analysis of viscoelastic cantilever carbon nanotubes conveying fluid. Comput Mater Sci 114:151–159

Bahaadini R, Hosseini M (2016b) Nonlocal divergence and flutter instability analysis of embedded fluid-conveying carbon nanotube under magnetic field. Microfluid Nanofluid 20:1–14

Bahaadini R, Hosseini M, Jamali B (2017a) Flutter and divergence instability of supported piezoelectric nanotubes conveying fluid. Physica B. https://doi.org/10.1016/j.physb.2017.09.130

Bahaadini R, Hosseini M, Jamalpoor A (2017b) Nonlocal and surface effects on the flutter instability of cantilevered nanotubes conveying fluid subjected to follower forces. Physica B 509:55–61. https://doi.org/10.1016/j.physb.2016.12.033

Beskok A, Karniadakis GE (1999) Report: a model for flows in channels, pipes, and ducts at micro and nano scales. Microscale Thermophys Eng 3:43–77

Bianco A, Kostarelos K, Prato M (2005) Applications of carbon nanotubes in drug delivery. Curr Opin Chem Biol 9:674–679

Che G, Lakshmi BB, Fisher ER, Martin CR (1998) Carbon nanotubule membranes for electrochemical energy storage and production. Nature 393:346–349

Chen T, Su GY, Shen YS, Gao B, Li XY, Müller R (2016) Unified Green's functions of forced vibration of axially loaded Timoshenko beam: transition parameter. Int J Mech Sci 113:211–220. https://doi.org/10.1016/j.ijmecsci.2016.05.003

Duan W, Wang C, Zhang Y (2007) Calibration of nonlocal scaling effect parameter for free vibration of carbon nanotubes by molecular dynamics. J Appl Phys 101:024305

Ghannadiasl A, Mofid M (2016) Free vibration analysis of general stepped circular plates with internal elastic ring support resting on Winkler foundation by green function method. Mech Based Des Struct Mach 44:212–230. https://doi.org/10.1080/15397734.2015.1051228

Ghavanloo E, Fazelzadeh SA (2011) Flow-thermoelastic vibration and instability analysis of viscoelastic carbon nanotubes embedded in viscous fluid. Physica E 44:17–24

Ghavanloo E, Fazelzadeh SA (2016) Evaluation of nonlocal parameter for single-walled carbon nanotubes with arbitrary chirality. Meccanica 51:41–54

Ghorbanpour Arani A, Bagheri MR, Kolahchi R, Khoddami Maraghi Z (2013) Nonlinear vibration and instability of fluid-conveying DWBNNT embedded in a visco-Pasternak medium using modified couple stress theory. J Mech Sci Technol 27:2645–2658. https://doi.org/10.1007/s12206-013-0709-3

Gogotsi Y (2010) High-temperature rubber made from carbon nanotubes. Science 330:1332–1333. https://doi.org/10.1126/science.1198982

Habibi S, Hosseini M, Izadpanah E, Amini Y (2016) Applicability of continuum based models in designing proper carbon nanotube based nanosensors. Comput Mater Sci 122:322–330

Hosseini M, Sadeghi-Goughari M (2016) Vibration and instability analysis of nanotubes conveying fluid subjected to a longitudinal magnetic field. Appl Math Model 40:2560–2576. https://doi.org/10.1016/j.apm.2015.09.106

Hosseini M, Sadeghi-Goughari M, Atashipour S, Eftekhari M (2014) Vibration analysis of single-walled carbon nanotubes conveying nanoflow embedded in a viscoelastic medium using modified nonlocal beam model. Arch Mech 66:217–244

Hosseini M, Bahaadini R, Jamali B (2016a) Nonlocal instability of cantilever piezoelectric carbon nanotubes by considering surface effects subjected to axial flow. J Vib Control. https://doi.org/10.1177/1077546316669063

Hosseini M, Bahreman M, Jamalpoor A (2016b) Thermomechanical vibration analysis of FGM viscoelastic multi-nanoplate system incorporating the surface effects via nonlocal elasticity theory. Microsyst Technol. https://doi.org/10.1007/s00542-016-3133-7

Hosseini M, Bahreman M, Jamalpoor A (2016c) Using the modified strain gradient theory to investigate the size-dependent biaxial buckling analysis of an orthotropic multi-microplate system. Acta Mech 227:1621–1643. https://doi.org/10.1007/s00707-016-1570-0

Hosseini M, Jamalpoor A, Bahreman M (2016d) Small-scale effects on the free vibrational behavior of embedded viscoelastic double-nanoplate-systems under thermal environment. Acta Astronaut 129:400–409. https://doi.org/10.1016/j.actaastro.2016.10.001

Hosseini M, Dini A, Eftekhari M (2017a) Strain gradient effects on the thermoelastic analysis of a functionally graded micro-rotating cylinder using generalized differential quadrature method. Acta Mech. https://doi.org/10.1007/s00707-016-1780-5

Hosseini M, Zandi Baghche Maryam A, Bahaadini R (2017b) Forced vibrations of fluid-conveyed double piezoelectric functionally graded micropipes subjected to moving load. Microfluid Nanofluid 21:134. https://doi.org/10.1007/s10404-017-1963-y

Hsieh J-Y, Lu J-M, Huang M-Y, Hwang C-C (2006) Theoretical variations in the Young's modulus of single-walled carbon nanotubes with tube radius and temperature: a molecular dynamics study. Nanotechnology 17:3920

Hu Y-G, Liew KM, Wang Q (2011) Nonlocal continuum model and molecular dynamics for free vibration of single-walled carbon nanotubes. J Nanosci Nanotechnol 11:10401–10407

Husson JM, Dubois F, Sauvat N (2011) A finite element model for shape memory behavior. Mech Time-Depend Mater 15:213–237. https://doi.org/10.1007/s11043-011-9134-0

Hwang K (2004) Thermal expansion of single wall carbon nanotubes. Urbana 51:61801

Jafari A, Bahaaddini R, Jahanbakhsh H (2017) Numerical analysis of peridynamic and classical models in transient heat transfer, employing Galerkin approach. Heat Transf Asian Res. https://doi.org/10.1002/htj.21317

Jamalpoor A, Ahmadi-Savadkoohi A, Hosseini M, Hosseini-Hashemi S (2017a) Free vibration and biaxial buckling analysis of double magneto-electro-elastic nanoplate-systems coupled by a visco-Pasternak medium via nonlocal elasticity theory. Eur J Mech A Solids 63:84–98. https://doi.org/10.1016/j.euromechsol.2016.12.002

Jamalpoor A, Bahreman M, Hosseini M (2017b) Free transverse vibration analysis of orthotropic multi-viscoelastic microplate system embedded in visco-Pasternak medium via modified strain gradient theory. J Sandw Struct Mater. https://doi.org/10.1177/1099636216689384
Jiang J-W, Wang J-S, Li B (2009) Thermal expansion in single-walled carbon nanotubes and graphene: Nonequilibrium Green's function approach. Phys Rev B 80:205429
Karlicic D, Murmu T, Adhikari S, McCarthy M (2015) Non-local structural mechanics. Wiley, New York
Karniadakis G, Beskok A, Aluru N (2005) Simple fluids in nanochannels. Springer, Berlin
Kiani K (2013) Vibration behavior of simply supported inclined single-walled carbon nanotubes conveying viscous fluids flow using nonlocal Rayleigh beam model. Appl Math Model 37:1836–1850. https://doi.org/10.1016/j.apm.2012.04.027
Kukla S, Zamojska I (2007) Frequency analysis of axially loaded stepped beams by Green's function method. J Sound Vib 300:1034–1041. https://doi.org/10.1016/j.jsv.2006.07.047
Lassagne B, Garcia-Sanchez D, Aguasca A, Bachtold A (2008) Ultrasensitive mass sensing with a nanotube electromechanical resonator. Nano Lett 8:3735–3738
Lei ZX, Liew KM, Yu JL (2013) Free vibration analysis of functionally graded carbon nanotube-reinforced composite plates using the element-free kp-Ritz method in thermal environment. Compos Struct 106:128–138. https://doi.org/10.1016/j.compstruct.2013.06.003
Li Y-d, Yang Y-r (2014) Forced vibration of pipe conveying fluid by the Green function method. Arch Appl Mech 84:1811–1823
Li XY, Zhao X, Li YH (2014) Green's functions of the forced vibration of Timoshenko beams with damping effect. J Sound Vib 333:1781–1795. https://doi.org/10.1016/j.jsv.2013.11.007
Liu Y, Chen X (2003) Continuum models of carbon nanotube-based composites using the boundary element method. Electr J Bound Elem 1:316–335
Liu Y, Nishimura N, Otani Y (2005) Large-scale modeling of carbon-nanotube composites by a fast multipole boundary element method. Comput Mater Sci 34:173–187
Liu YJ, Nishimura N, Qian D, Adachi N, Otani Y, Mokashi V (2008) A boundary element method for the analysis of CNT/polymer composites with a cohesive interface model based on molecular dynamics. Eng Anal Bound Elem 32:299–308. https://doi.org/10.1016/j.enganabound.2007.11.006
Mattia D, Gogotsi Y (2008) Review: static and dynamic behavior of liquids inside carbon nanotubes. Microfluid Nanofluid 5:289–305
Mehdipour A, Sebak AR, Trueman CW (2012) Green's function of a dielectric slab grounded by carbon fiber composite materials. IEEE Trans Electromagn Compat 54:118–125. https://doi.org/10.1109/TEMC.2011.2174996
Mirramezani M, Mirdamadi HR (2012) Effects of nonlocal elasticity and Knudsen number on fluid–structure interaction in carbon nanotube conveying fluid. Physica E 44:2005–2015
Mirzaei M, Kiani Y (2016) Free vibration of functionally graded carbon-nanotube-reinforced composite plates with cutout. Beilstein J Nanotechnol 7:511
Mohammadimehr M, Mohammadi-Dehabadi AA, Maraghi ZK (2017) The effect of non-local higher order stress to predict the nonlinear vibration behavior of carbon nanotube conveying viscous nanoflow. Physica B 510:48–59. https://doi.org/10.1016/j.physb.2017.01.014
Narendar S, Gopalakrishnan S (2011) Spectral finite element formulation for nanorods via nonlocal continuum mechanics. J Appl Mech 78:061018–061019. https://doi.org/10.1115/1.4003909
Nicholson JW, Bergman LA (1986) Free vibration of combined dynamical systems. J Eng Mech 112:1–13
Qian D, Zhou Z (2011) Visco-elastic properties of carbon nanotubes and their relation to damping. In: Proulx T (ed) Time dependent constitutive behavior and fracture/failure processes, vol 3, Proceedings of the 2010 annual conference on experimental and applied mechanics. Springer, New York, pp 259–265. https://doi.org/10.1007/978-1-4419-9794-4_36
Rashidi V, Mirdamadi HR, Shirani E (2012) A novel model for vibrations of nanotubes conveying nanoflow. Comput Mater Sci 51:347–352
Rezania H, Daneshfar N (2012) Study of third-harmonic generation in zigzag carbon nanotubes using the Green function approach. Appl Phys A 109:503–508. https://doi.org/10.1007/s00339-012-7063-7
Sadeghi-Goughari M, Hosseini M (2015) The effects of non-uniform flow velocity on vibrations of single-walled carbon nanotube conveying fluid. J Mech Sci Technol 29:723–732. https://doi.org/10.1007/s12206-015-0132-z
SafarPour H, Ghadiri M (2017) Critical rotational speed, critical velocity of fluid flow and free vibration analysis of a spinning SWCNT conveying viscous fluid. Microfluid Nanofluid 21:22. https://doi.org/10.1007/s10404-017-1858-y
Sazonova V, Yaish Y, Üstünel H, Roundy D, Arias TA, McEuen PL (2004) A tunable carbon nanotube electromechanical oscillator. Nature 431:284–287
Scarpa F, Boldrin L, Peng H-X, Remillat C, Adhikari S (2010) Coupled thermomechanics of single-wall carbon nanotubes. Appl Phys Lett 97:151903
Shames IH, Shames IH (1982) Mechanics of fluids, vol 2. McGraw-Hill, New York
Shokouhmand H, Isfahani AM, Shirani E (2010) Friction and heat transfer coefficient in micro and nano channels filled with porous media for wide range of Knudsen number. Int Commun Heat Mass Transf 37:890–894
Sweilam NH, Khader MM (2010) Approximate solutions to the nonlinear vibrations of multiwalled carbon nanotubes using Adomian decomposition method. Appl Math Comput 217:495–505. https://doi.org/10.1016/j.amc.2010.05.082
Tiwari A (2013) Innovative graphene technologies: evaluation and applications, vol 2. Smithers Rapra, Shrewsbury
Tserpes KI, Papanikos P (2005) Finite element modeling of single-walled carbon nanotubes. Compos B Eng 36:468–477. https://doi.org/10.1016/j.compositesb.2004.10.003
Wang Q, Varadan VK, Quek ST (2006) Small scale effect on elastic buckling of carbon nanotubes with nonlocal continuum models. Phys Lett A 357:130–135. https://doi.org/10.1016/j.physleta.2006.04.026
Wang C, Zhang Y, He X (2007) Vibration of nonlocal Timoshenko beams. Nanotechnology 18:105401
Wang L, Hong Y, Dai H, Ni Q (2016) Natural frequency and stability tuning of cantilevered CNTs conveying fluid in magnetic field. Acta Mech Solida Sin 29:567–576. https://doi.org/10.1016/S0894-9166(16)30328-7
Xia W, Wang L (2010) Microfluid-induced vibration and stability of structures modeled as microscale pipes conveying fluid based on non-classical Timoshenko beam theory. Microfluid Nanofluid 9:955–962. https://doi.org/10.1007/s10404-010-0618-z
Xu M, Futaba DN, Yamada T, Yumura M, Hata K (2010) Carbon nanotubes with temperature-invariant viscoelasticity from −196° to 1000 °C. Science 330:1364–1368. https://doi.org/10.1126/science.1194865
Yakobson BI, Brabec C, Bernholc J (1996) Nanomechanics of carbon tubes: instabilities beyond linear response. Phys Rev Lett 76:2511
Yan W, Mortensen NA, Wubs M (2013) Green's function surface-integral method for nonlocal response of plasmonic nanowires in arbitrary dielectric environments. Phys Rev B (Condens Matter Mater Phys) 88:155414. https://doi.org/10.1103/PhysRevB.88.155414
Yang W, Thordarson P, Gooding JJ, Ringer SP, Braet F (2007) Carbon nanotubes for biological and biomedical applications. Nanotechnology 18:412001

Yao X, Han Q (2008) A continuum mechanics nonlinear postbuckling analysis for single-walled carbon nanotubes under torque. Eur J Mech A Solids 27:796–807

Zeighampour H, Beni YT, Karimipour I (2017) Wave propagation in double-walled carbon nanotube conveying fluid considering slip boundary condition and shell model based on nonlocal strain gradient theory. Microfluid Nanofluid 21:85. https://doi.org/10.1007/s10404-017-1918-3

Zhang Z, Liu Y, Zhao H, Liu W (2016) Acoustic nanowave absorption through clustered carbon nanotubes conveying fluid. Acta Mech Solida Sin 29:257–270. https://doi.org/10.1016/S0894-9166(16)30160-4

Zhang Y-W, Zhou L, Fang B, Yang T-Z (2017) Quantum effects on thermal vibration of single-walled carbon nanotubes conveying fluid. Acta Mech Solida Sin. https://doi.org/10.1016/j.camss.2017.07.007

Zhao X, Yang EC, Li YH (2015) Analytical solutions for the coupled thermoelastic vibrations of Timoshenko beams by means of Green′s functions. Int J Mech Sci 100:50–67. https://doi.org/10.1016/j.ijmecsci.2015.05.022

Zhao X, Zhao YR, Gao XZ, Li XY, Li YH (2016) Green′s functions for the forced vibrations of cracked Euler–Bernoulli beams. Mech Syst Signal Process 68–69:155–175. https://doi.org/10.1016/j.ymssp.2015.06.023

Zhou Z, Qian D, Yu M-F (2011) A computational study on the transversal visco-elastic properties of single walled carbon nanotubes and their relation to the damping mechanism. J Comput Theor Nanosci 8:820–830